Received: 27 July 2019 | Revised: 19 September 2019 | Accepted: 29 October 2019

DOI: 10.1002/qua.26107

FULL PAPER

International Journal of QUANTUM CHEMISTRY WILEY

The effects of Zn^{2+} and ClO_4^- in the excellent primary explosive $Zn(CHZ)_3(ClO_4)_2$

Kun Wang[1,2] | Chaohua Dai[1] | Chen Sun[1] | Longjiu Cheng[1] | Jianguo Zhang[3] | Tonglai Zhang[3]

[1]Department of Chemistry, Anhui University, Hefei, Anhui, China

[2]Department of Materials Science, Fudan University, Shanghai, China

[3]State Key Laboratory of Explosion Science and Technology, Beijing Institute of Technology, Beijing, China

Correspondence
Kun Wang, Department of Chemistry, Anhui University, Hefei, Anhui 230601, China.
Email: wangkun@ahu.edu.cn
Tonglai Zhang, State Key Laboratory of Explosion Science and Technology, Beijing Institute of Technology, Beijing 100081, China.
Email: ztlbit@bit.edu.cn

Funding information
China Postdoctoral Science Foundation, Grant/Award Number: 2018M632013; National Natural Science Foundation of China, Grant/Award Number: 21701001; Natural Science Foundation of Anhui Province, Grant/Award Number: 1708085QB42

Abstract

Metal carbohydrazide perchlorates ($M(CHZ)_3(ClO_4)_2$, simplified as MCP, M = alkali earth metals, Mn, Fe, Co, Ni, Cu, Zn, and Cd) are a series of stable and high-energetic compounds, in which ZnCP as an environment-friendly and high energetic primary explosive has been applied broadly in recent 10 years. Based on the traditional viewpoints, the cleavage of Zn-N coordinative bond initializes the decomposition, where the perchlorate is only an oxidizing agent in ZnCP. However, by applying CPMD method, we prove the decomposition is not only from the cleavage of coordinative bond, but also with the synergetic homolysis of the Cl-O bond of perchlorate. We find the relationship between the explosive performance and the centre metal in ZnCP. The electronic structure suggests Zn^{2+} is a stabilizer in the complex under the ambient condition. But in the decomposition, Zn^{2+} is a catalyst and an anion-carrier in the explosion. For ZnCP, the initial process of the decomposition proceeds as the synergetic oxygen transferring mechanism, but it is a stepwise ring-opening mechanism in the deflagration to detonation transition process. The total explosion pathways of ZnCP are descripted in our simulation.

KEYWORDS

carbohydrazide, Car-PARRINELLO molecular dynamics, primary explosive, zinc carbohydrazide perchlorate

1 | INTRODUCTION

The traditional primary explosives containing heavy metal such as lead azide, lead styphnate, or mercury fulminate have been washed out caused by their environmental pollution and very dangerous mechanic sensitivity.[1–4] There is a new series of energetic complexes containing the ligand of carbohydrazide (, CHZ) with the external anion of perchlorate attracts many attentions in recent 10 years.[5–7] From 1988 to 2010, Sinditskii and Zhang et al. synthesized the transitional metallic carbohydrazide perchlorate (including Mn, Co, Ni, Zn, Cd, and Cu) and studied their structures, thermal properties, sensitivities, and explosive properties.[8–14] ZnCP and CdCP appear the best explosive performances, which have been generalized into the application in the industry based on the Talawar's research.[11]

Zinc carbohydrazide perchlorate (ZnCP, or named GTX in industry) is a kind of environment-friendly energetic primary explosives with acceptable thermal stability, excellent fluidity and high density, which is synthesized by mixing CHZ and aqueous $Zn(ClO_4)_2$ with the molar ratio of 3:1 under 80°C.[9] ZnCP is different from the other compounds of metallic carbohydrazide perchlorate (MCP, M = alkali earth metals, Mn, Fe, Co, Ni, Cu, Zn, Cd),[15] although all the MCP complexes appear the similar coordination pathways between the centre metals and the energetic ligands. The initial decomposition temperature of most of them are above 240°C except CuCP (120°C) and FeCP (152.7°C).[14] As for ZnCP, there are intensive continuous exothermic decomposition processes at 280~340°C. This indicates its excellent thermal stability at normal condition and

excellent energetic characters in the explosion. Base on the experimental structure,[9] the three carbohydrazides as three bidentate ligands coordinate with Zn^{2+} through the oxygen atoms in carbonyl groups and the terminal nitrogen atoms to form three 5-membered rings, while two perchlorate anions balance the charges of center metal cation by Column interaction. The previous research indicates there are a large number of intramolecular hydrogen bonds in the structure to stabilize the structure efficiently.[11,14] The DSC analysis of ZnCP indicates it is stable before heating to 270°C. The main product in the decomposition is predicted as ZnO based on the experiment.[9]

As for its already application in the industry field and its excellent performances in the explosion, it should be an interesting topic to understand what is the role of Zn^{2+} and ClO_4^- in the equilibrium state and the decomposition. We applied CPMD method to simulate the explosion by rising the temperature continuously to understand all the pathways in the process. This will help us to understand the speciality of ZnCP in the family of MCP primary explosives.

2 | METHOD

There are five coordination positions in each molecular CHZ, we first discuss all the possible structures with different coordination pathways between Zn^{2+} and CHZ in gas phase. All of them are optimized and analyzed under the level of BP86 with the basis set of 6-31+G(d,p) for C/H/O/N atoms and Lanl2dz for Zn[16,17] in Gaussian 09 package[18] (Figure 1).

The optimization and electronic structure of crystal ZnCP is implemented in CASTEP program[19] based on the experimental XRD data.[9] The GGA-PBE approximation is used for the exchange-correlation function in the optimization.[20] The PBE-type ultrasoft pseudopotentials with valence states Zn ($3d^{10}4s^2$), C($2s^22p^2$), N($2s^22p^3$), O($2s^22p^1$), and H($1s^1$) were used to describe the core electrons. The $4 \times 4 \times 2$ Monkhorst-Pack meshes[21] are used for the Brillouin-zone integration in the optimization. A plane wave basis set with the cut-off energy of 550 eV has been used. Structural relaxations including atomic positions, cell structures were carried out by BFGS method[22] until the residual forces and stresses were less than 0.005 eV/Å and 0.05 Gpa. The optimized structures have been showed in Figure 2. The HSE06 functional are applied to calculate the electronic properties based on the optimized crystal structure.

All the dynamic calculations were performed with Quantum Espresso 6.0 package.[23] We accomplish CPMD calculations[24] on the basis of the optimized unit cell after making *P*1 symmetry. The time step is set as 4.0 a.u. (~0.1 fs) in the simulation. The kinetic energy cutoff for wave functions is 40 Ry (544 eV) with the effective electron mass of 600 a.u. The PBE exchange-correlation functional was chosen, and core electrons are taken into account using PBE-type ultrasoft pseudopotentials, for which the dimension of the grid is $21 \times 21 \times 21$. In the simulation of CPMD, the duration of the simulation was set as ~62.5 ps (around 625 000 steps). The oscillation frequency of the Noše thermostat[25] is set as 600 THz. An NVT ensemble (keep number-volume-temperature as constants) was employed for the simulation box and the external temperature was gradually increased by an increment of 100 K at the range of 100~3000 K. The extra high temperature is set for accelerate the decomposition, so that we can possibly observe all the decomposition pathways in the finite time simulation. The time of the simulation for each step has been set as 1~5 ps (10 000~50 000 steps) for reaching the balanced system under the corresponding temperature. We keep studying the decomposition in ~62.5 ps including 625 000 steps in total. The reaction energies are analyzed by M06-2x/6-311 + G(d,p)[16] theoretical level in Gaussian 09 program based on the results of CPMD simulation.

3 | RESULTS AND DISCUSSIONS

3.1 | The coordination environment of $[Zn(CHZ)_3]^{2+}$

Based on the single-crystal structure,[9] three ligands coordinate with Zn^{2+} through N1 and O3 atoms (Figure 1B). In the complex, Zn^{2+} adopts sp^3d^2 hybridization to provide six empty degenerate orbitals in the structure. As for the ligands, N1 and N5 atoms adopt sp^3 hybridization. N2, N4, C6, and O3 atoms adopt sp^2 hybridization. Theoretically, all the N1/N2/O3/N4/N5 atoms in molecular CHZ are the potential coordination sites in the complex (labeled in Figure 1, CHZ) caused by their abilities of donating lone electron pairs to the centre anion.

We calculated six possible coordination modes (A-F showed in Figure 1) between Zn^{2+} and CHZ ligands to understand the most stable coordination structure.[9] In the calculation, CHZ is considered as the bidentate ligand, where they coordinate with Zn^{2+} through the same two coordination atoms. We optimized their structures to compare their typical bond lengths, atomic charges, and Wiberg bond index (WBI), which is showed in Figure 1. The total electronic energies of the six compounds are showed in Table 1, where B appears the lowest electronic energy, suggesting its highest chemical stability, which is consistent with the experiment very well. In structure B, Zn-N1-N2-C6-O3 forms a planar five-membered ring with the dihedral of 4° of N1-Zn-O3-C6. Except the angle of N1-Zn-O3 (77°), the other bond angle including Zn-O3-C6, O3-C6-N2, and C6-N2-N1 are all around 120°. The bond lengths of the ligands are averaged after the coordination, suggesting the conjugative effect among N1/Zn/O3/C6 decrease the electronic energy of the structure.

The stability of B should be related to this five-membered ring with the strongest conjugative effect (5c-4e bond) among the six structures. For A, it is a triangle structure of N1-Zn-N2, leading to the polarized charge distribution in the complex. E is a four-membered ring with a weaker

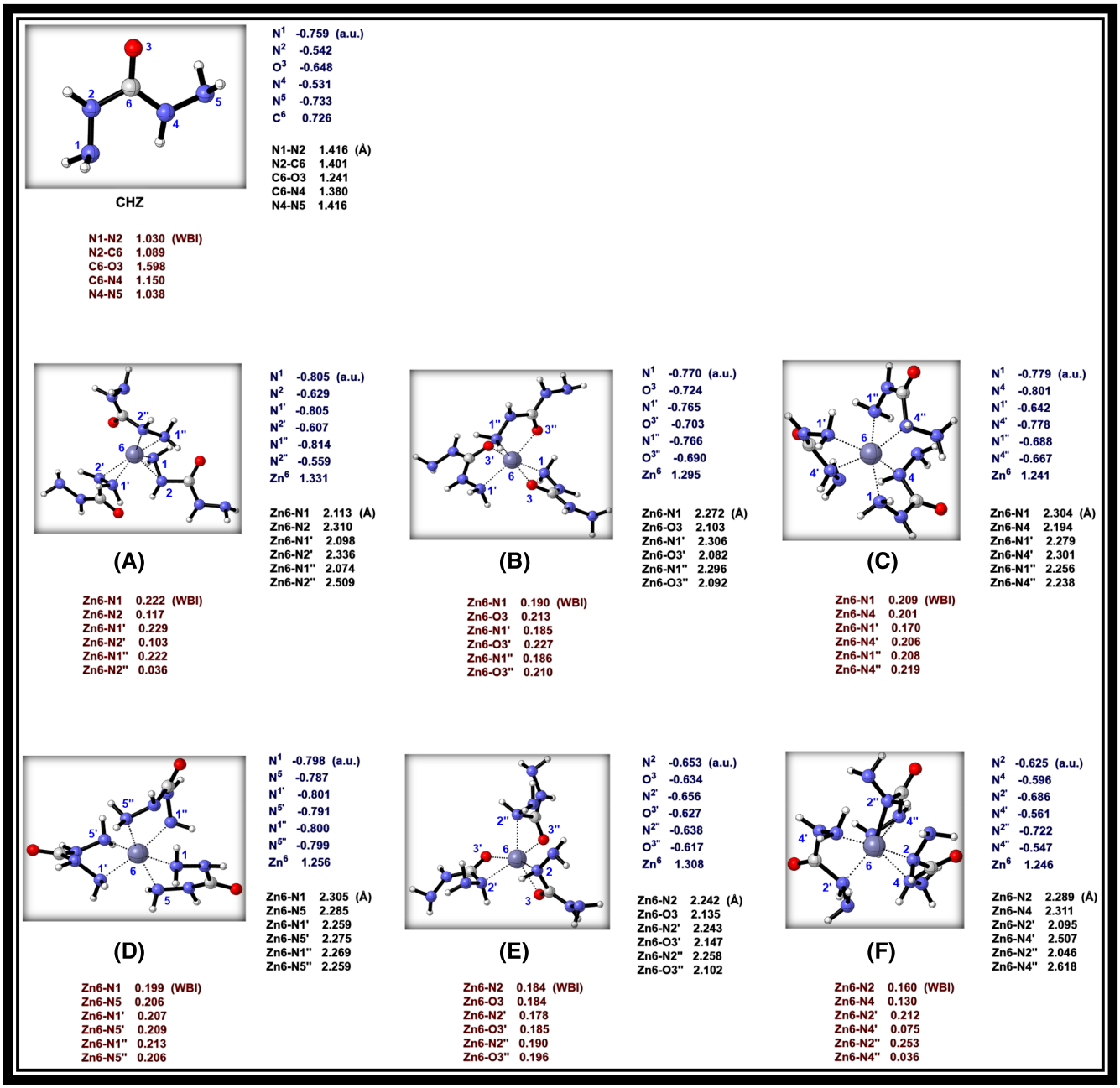

FIGURE 1 The optimized six isomers of $[Zn(CHZ)]^{2+}$ with the corresponding bond lengths, NBO atomic charges, and Wiberg bond index of the coordination bonds (WBI). The optimized CHZ and the atom labels are boxed on the upper left. Purple: Zn, Blue: N, Red: O, Gray: C, White: H

conjugative effect compared with that of B. In the structure C, D, and F, the carbonyl group is between the coordination bonds, where the electron-withdrawing effect of the carbonyl group (Compare with B, the atomic charges of N and Zn both decreased) weakens the conjugative effect and increase the electronic energy.

We calculate the reaction Gibbs free energies for the six isomers based on the corresponding synthesis reactions[9] of Zn^{2+} + 3CHZ → $[Zn(CHZ)_3]^{2+}$, where the results are listed in Table 1. The formation of B decreases the chemical potential the most in the six reactions. Therefore, B is the most stable conformation because of its delocalized 5c-4e bond, which appears the lowest chemical potential as the product of the synthesized reaction.

As showed as Figure 1B, the WBI indicates Zn-N bond is the weakest bond in the compound, even weaker than that of Zn-O bond. So theoretically, the cleavage of Zn-N bond triggers the decomposition. The differences among the three WBI values of Zn-N bonds (0.19/0.185/0.186). The calculated bond dissociation energy (BDE) of the first Zn-N coordinative bond in $[Zn(CHZ)_3]^{2+}$ is 28.3 kcal/mol. The second and the third

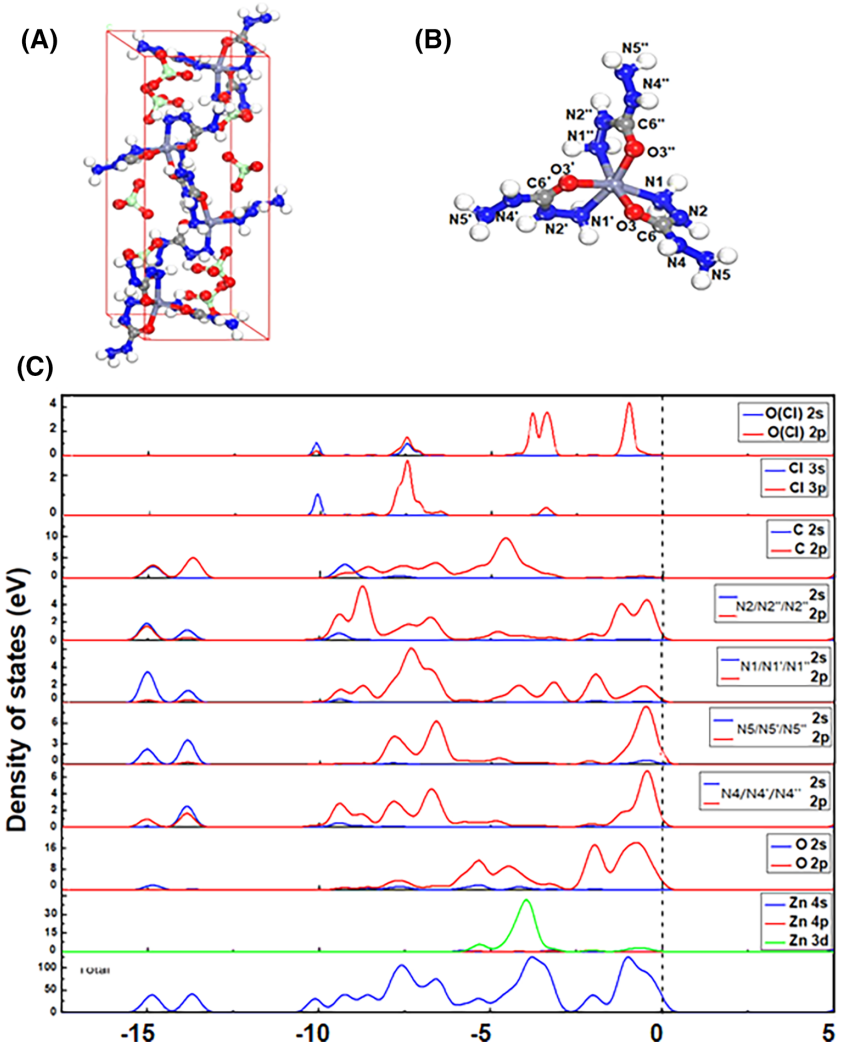

FIGURE 2 A, The optimized structure of crystalline ZnCP; B, The conformation of molecular $[Zn(CHZ)_3]^{2+}$ in the crystal with the labels at the corresponding atoms; C, The total and partial density of states (DOS and pDOS) of ZnCP

$[Zn(CHZ)_3]^{2+}$	A	B	C	D	E	F
E_{tot}	55.1	0[a]	65.5	74	55.2	115.6
$\Delta_f G_m^{\ominus}$	−262.84	−324.43	−243.96	−243.79	−257.52	−200.26

[a]We set the total electronic energy of B as zero for the comparison in B to F.

TABLE 1 The total electronic energy E_{tot} and formation Gibbs free energies for the six isomers of complex ions (kcal/mol)

BDEs of Zn-N bonds in $[Zn(CHZ)_2]^{2+}$ and $[Zn(CHZ)]^{2+}$ are 20.7 kcal/mol and 12.7 kcal/mol. Both the WBI results and BDEs are suggesting the three Zn-N bonds break stepwisely in the decomposition.

3.2 | Optimized structure of crystalline ZnCP

The crystal parameters are calculated as a = 10.04 Å (10.00 Å), b = 8.55 Å (8.43 Å), c = 21.35 Å (21.22 Å), β = 100.8° (100.9°), where the results in the brackets are from the experiment. In crystalline ZnCP, each Zn^{2+} coordinates to three CHZ groups through N3/N3′/N3″ and O1/O1′/O1″ (d(Zn-N1) = 2.17 Å, d(Zn-O3) = 2.17 Å, ∠(N2-Zn-O1) = 77.3°) with P_{21}/N symmetry and *monoclinic* syngony (Figure 2A,B). Compared with the gas-phase structure in Figure 1, the typical bond lengths in the five-membered ring are further averaged in the crystal structure caused by the Madelung's energy and the Coulomb's interaction.

The electronic populations for Zn-O3 and Zn-N1 bonds are 0.19 and 0.12, respectively, which is consistent with the results of the gas-phase structure, where Zn-N bond is more stable than that of Zn-O bond. The results of electronic population are similar with that of the WBI analysis for molecular CHZ.

We design three-step reactions for obtaining the energies of the stepwise ring-opening Zn-$(CHZ)_3$ group as: $[Zn\text{-}(CHZ)_3]^{2+} \rightarrow [Zn\text{-}(CHZ)_2]^{2+}$ + CHZ, $[Zn\text{-}(CHZ)_2]^{2+} \rightarrow [Zn\text{-}(CHZ)]^{2+}$ + CHZ and $[Zn\text{-}(CHZ)]^{2+} \rightarrow Zn^{2+}$ + CHZ. All the structures of the ring-opening reactions are optimized based on the solid ground-state ZnCP with the same theoretical level, where we only calculate one molecule in the cell with freezing all the other atoms. The molecular CHZ are optimized in a cell of 30 × 30 × 30 Å. The energy of the first ring-opening is −149 kcal/mol. However, the second and the third ring-opening reactions are endothermically, with the energies of 143 and 62 kcal/mol, which suggest it is more stable for $[Zn\text{-}(CHZ)_2]^{2+}$ than that of $[Zn\text{-}(CHZ)_3]^{2+}$. The different reaction energies further suggest the stepwise mechanism in the decomposition.

We applied HSE06 functional to calculate the total and partial density of states (DOS and pDOS) for ZnCP as showed in Figure 2C. The band gap of ZnCP is 5.02 eV, indicating its insulativity and stability. There are two energy regions of the valence electronic states from −20 ~ 0 eV. In the lowest energy region, the energy bands at around −15 eV are mainly composed of C/N 2 seconds and 2p states with few contributions of O 2 seconds states. The top of the valence bands (−12 ~ 0 eV) are mainly composed of C 2p, N 2p, O 2p, and Zn 3d states, and of small part of O 2 seconds states, indicating the covalent properties of C-N, Zn-O, and Zn-N bonds. The overlap of the pDOS suggests there are more covalence components in Zn-O1 bond compare with that of Zn-N2 bond. The covalence characters between Cl and O(Cl) atom can be found in DOS around −6~ −8 eV. The overlap of Zn 3d and O(Cl) 2p electrons around −4 eV indicates there are obvious covalence components between Zn and O(Cl) atom except for the Coulomb's interaction. The results of electronic population and DOS analysis both indicate the weakest bond is Zn-N1, which should be the bond to trigger the continuous explosion in the decomposition.

3.3 | The thermal decomposition of solid ZnCP

Based on the optimized structure of ZnCP, we apply CPMD method to study its decomposition mechanism with the increased temperature. To satisfy the requirements of the simulation, we test and confirm the virtual mass of electronics (600 a.u.) and the cut off energy (40 Ry, around 544 eV) to make sure the system is adiabatic with an appropriate force field for all the atoms. The atomic force field are listed in Table S1. The temperature of ions, kinetic energies of virtual electrons and the total electronic energies are converged in a 1000-step energy initiation before rising temperature for the system. All the relative results of tests are showed in Figure S1.

3.3.1 | The synergetic O transferring mechanism in the initiation of the decomposition

As showed in Scheme 1, the decomposition starts from the splitting of Cl-O bond, which is different from our hypothesis based on the analysis of population. The population of Zn-N/Zn-O bond is 0.12/0.19. However, the population of Cl-O bond is 0.42, appearing higher stability than that of Zn-O/Zn-N bonds. There is no doubt that Zn-N bond is the weakest bond in the structure. It vibrates dramatically and even breaks at 42.6684 ps (2200 K). However, there are no new fragments or new radical generated with the vibration of Zn-N bonds. As descripted in Scheme 2, we find it is a reversible process of splitting and reconnection of Zn-N bond.

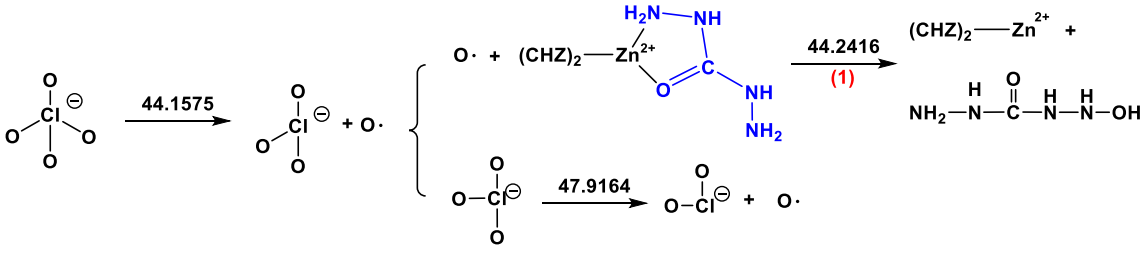

SCHEME 1 The splitting of Cl-O bond triggers the decomposition. The number showed on the arrows are suggesting the first formation time of the corresponding structure

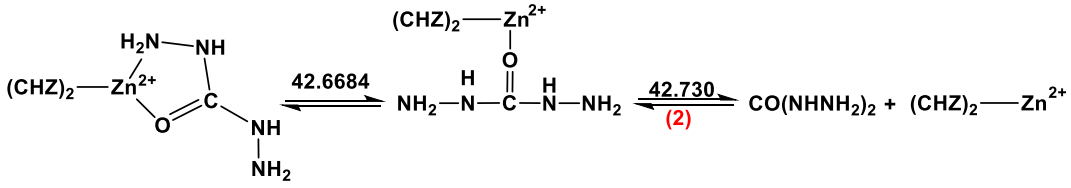

SCHEME 2 The reversible process of splitting and reconnection of Zn-N bond before the decomposition

Actually, the departure of a CHZ ligand suggests the decomposition. At 44.1575 ps (2200 K), we first observe the breaking of Cl-O. Then O radical as an attacking group gets close to the terminal N-H through H atom of one of the CHZ ligand, resulting in the synergetic bond cleavages of Zn-N bond and Zn-O bond, corresponding to the ring-opening and the departure of one ligand.

We compare the reaction Gibbs free energies of the first ring-opening reaction of (1) and (2) (highlighted in Schemes 1 and 2) by applying M06-2X method and 6-311+G(d,p) basis set. The ring-opening without O radical (Reaction (2)) requires the energy of 32.08 kcal/mol. However, it is only 4.69 kcal/mol for the reaction (1) catalyzed by O radical.

Therefore, the initiation is triggered by the splitting of Cl-O bond, which further catalysis the first ring-opening reaction with the splitting of Zn-N and Zn-O bonds synergetically. The sketch map of synergetic O transferring mechanism is showed as Figure 3.

3.3.2 | The stepwise mechanism in the explosion

It is stepwise mechanism for the three ligands dissociated from the center cation, where the three 5-membered rings open at 42.73 ps, 51.0281 ps, and 51.0358 ps, respectively. With the participation of O radical and ClO_4^- in the first ring-opening step, CHZ loses hydrogen radical successively started from the terminal N-H bond, where 2 equiv. H_2O are formed by the combination of H· and ·OH (Scheme 3). The enthalpies of H_2O-formation at 47.9996 and 48.5299 ps are −116.1 and −23.03 kcal/mol. The second combination of H· and ·OH is accompanied with the homolysis of the terminal N-H bond. The other two CHZ groups decompose as the similar way after the corresponding ring-opening reaction.

After completing the hemolysis of N-H bonds of CHZ, $[(CHZ)_2Zn]^{2+}$ as a Lewis acid interacts with the strong Lewis acid of to terminate the decomposition (Schemes 4 and 5). The combination of $[(CHZ)_2Zn]^{2+}$ and terminal N atom results in the charge redistribution in the structure, where N_2O is formed caused by the splitting of C-N bond with the enthalpy of −150.73 kcal/mol (49.9115 ps). With the participation of pre-formed H_2O, $[(CHZ)_2Zn]^{2+}$ transforms to $(CHZ)_2Zn(OH)_2$ caused by the Column interaction at 50.6120 ps (Scheme 4). Then the fragment of CHZ interacts with Cl^- and ClO_4^- to terminate the first decomposition process from 51.7934 ps to 51.7944 ps (initialized by the departure of the first

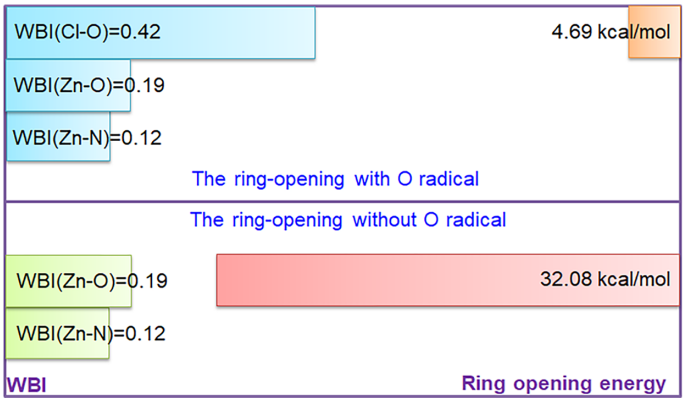

FIGURE 3 The sketch map of synergetic O transferring mechanism of ring-opening reaction

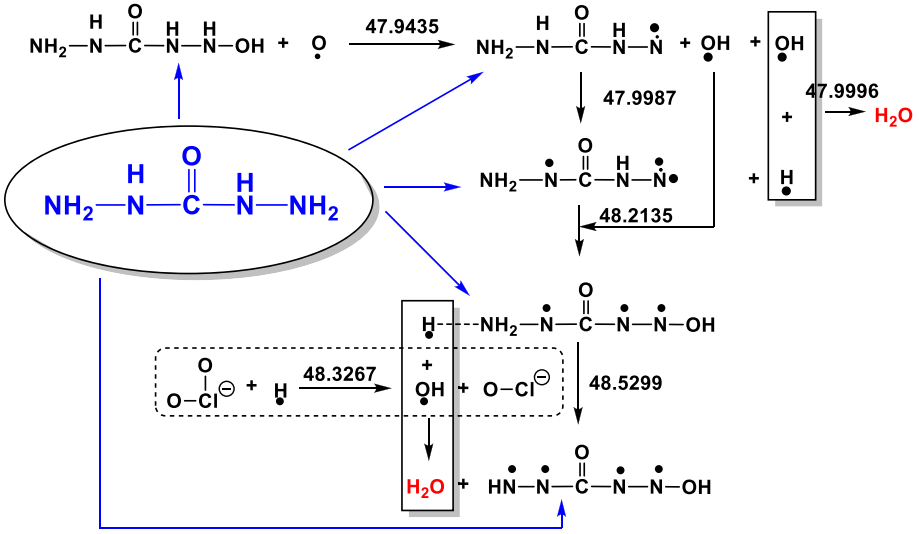

SCHEME 3 The cleavage of N-H bonds in CHZ groups

SCHEME 4 The role of Zn^{2+} played in the decomposition of CHZ

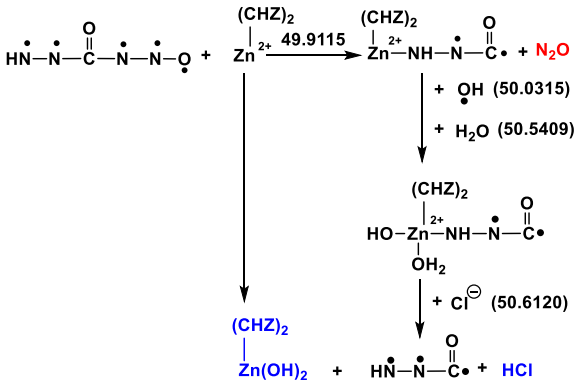

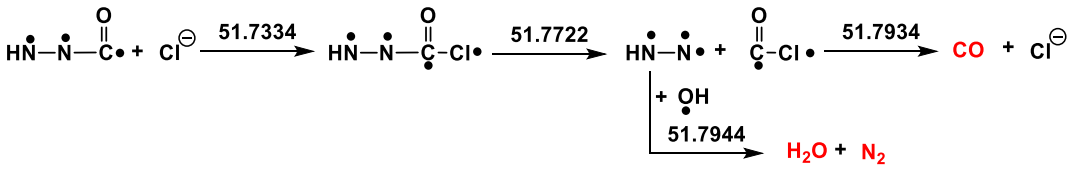

SCHEME 5 The first chain termination after the first departure of CHZ

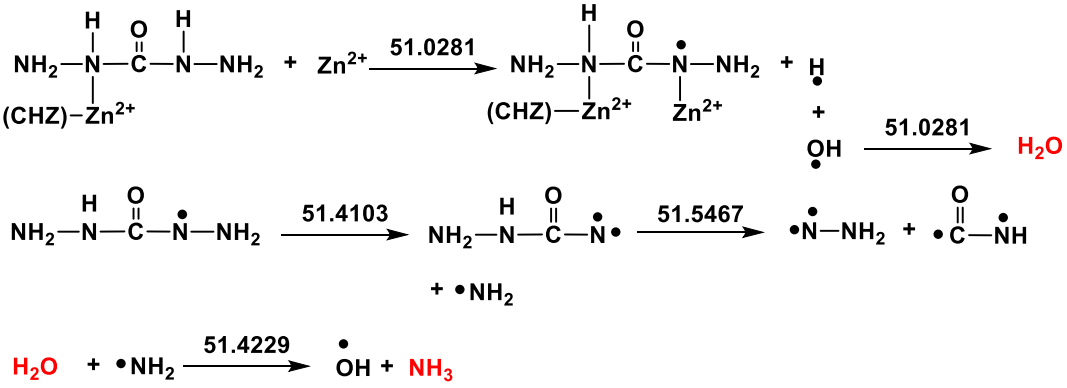

SCHEME 6 The departure of the second CHZ

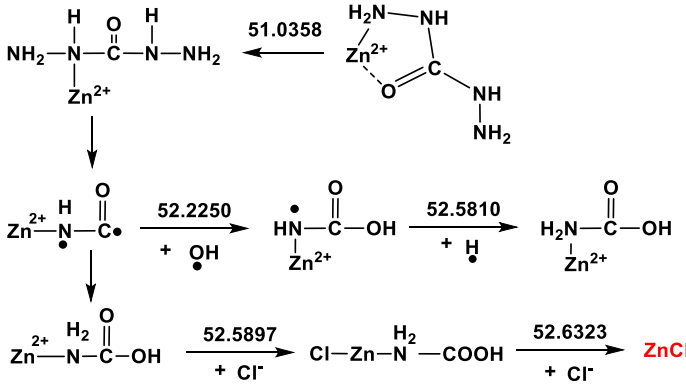

SCHEME 7 The termination of the decomposition

CHZ group, showed in Scheme 5). The enthalpies of formation of CO (51.7934 ps) and H_2O/N_2 (51.7944 ps) are −40.57 and − 222.63 kcal/mol (in Scheme 5).

As showed in Scheme 6, We observe the second ring-opening reaction of $[Zn(CHZ)_2]^{2+}$ triggered by the splitting of Zn-O bond at 51.0281 ps. Different from the first ring-opening reaction, the neighbored Zn^{2+} catalyzes the decomposition of the second CHZ group, rather than the catalysis of O radical. The generated H· combines with OH· to form water at 51.0281 ps with the enthalpy of −116.10 kcal/mol. We first find the

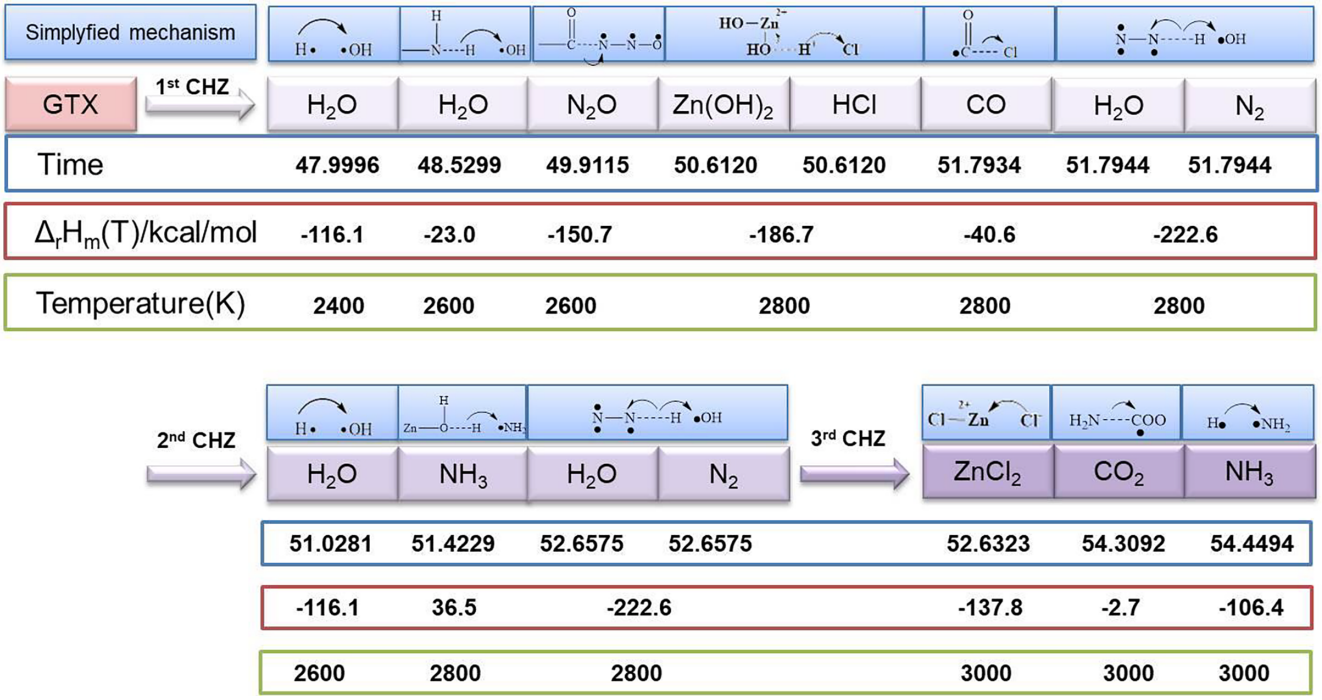

FIGURE 4 The typical intermediates and products in the three-step decomposition process with the corresponding mechanisms, and enthalpies, the time and temperature of their appearance

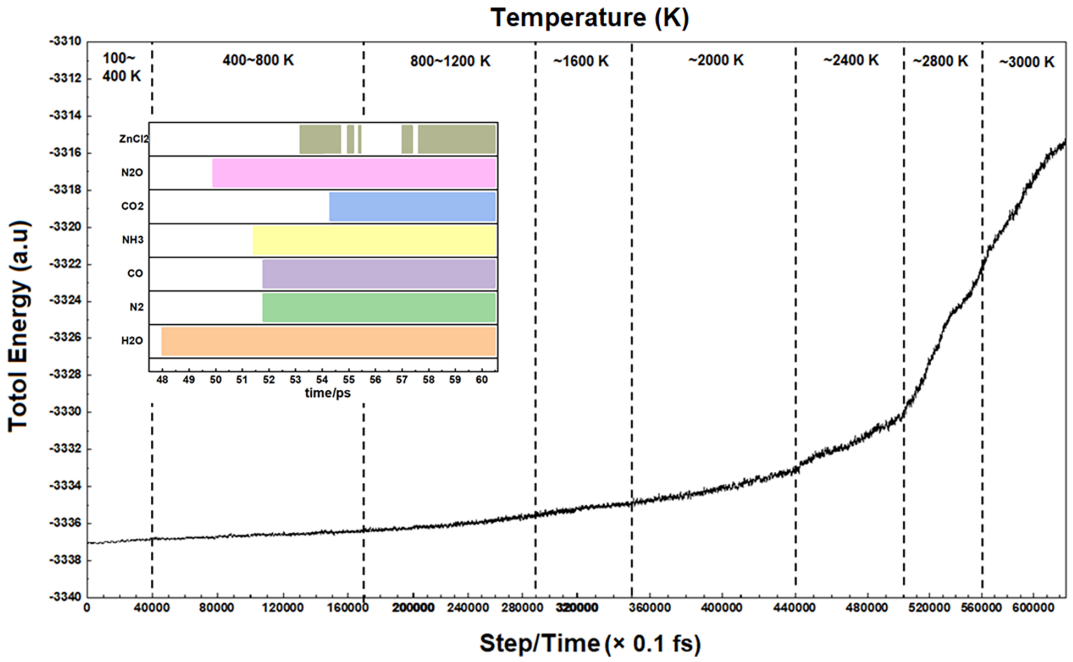

FIGURE 5 The relationship between the total energy and the simulation time (temperature). The lives of all the products are showed in the box

cleavage of N-N bond in CHZ's decomposition, results in the formation of -NH_2, which is further reacted with H radical to form NH_3 at 51.4229 ps. The positive enthalpy of reaction at 51.4229 ps (Scheme 6) is 36.5 kcal/mol. We observe the similar pathways in the generation of N_2, H_2O, and NH_3 in the decomposition of the second CHZ group, where the similar pathways can be found in Scheme 5.

At 51.0358 ps, we observe the last ring-opening reaction triggered by the cleavage of Zn-O bond. The cleavage of N-N bond and C-N bond generate the hydrazino group and amino group. With the participation of ClO_4^- and the hydrogen transferring, the final products are $ZnCl_2$, NH_3

and CO_2 (Scheme 7). We keep the temperature at 3000 K for another 5 ps (50 000 step), where we do not find any other new fragments produced. Therefore, we terminated the simulation at 3000 K. Different from the experimental speculation about the final product of Zn^{2+}.[9] We did not find the generation of ZnO and $Zn(OH)_2$ at the last 10 ps (100 000 steps). The final products in the decomposition are $ZnCl_2$, H_2O, NH_3, N_2, N_2O, CO, and CO_2. Based on the analysis of the simulation, the decomposition equation of ZnCP is as Equation (1).

$$Zn(N_2H_3\text{-}CO\text{-}N_2H_3)_3(ClO_4)_2 \rightarrow ZnCl_2 + 3H_2O + 4NH_3 + N_2 + 3N_2O + 2CO_2 + CO \quad (1)$$

It is the stepwise mechanism in the decomposition of ZnCP through three ring-opening steps (Figure 4). We summarize all the intermediates and products in the whole decomposition process, including the products, the simplified mechanisms, the formation time of products and their corresponding enthalpies (Three different colors in Figure 3). HCl and $Zn(OH)_2$ in the decomposition of the first step are the intermediates, which supply OH^-, H^+, and Cl^- as catalysts in the continuous decomposition. Some typical products are snapshotted from the simulation as showed in Figure S2.

The lives of all the products listed in Equation (1) are showed in the box of Figure 5. As showed in the bar chart, water is the main product generated from the first ring-opening step to the termination. The incontinuity of the life of $ZnCl_2$ is caused by temporary appearances of $Zn(OH)_2$ from 54 to 58 ps.

The relationship between the total energy and the simulation time (temperature) are showed in Figure 4. It is the process of deflagration to detonation transition from 36 to 56 ps in the simulation (2000-2800 K), which is initialized by the synergetically bond cleavage of both Zn-N and Cl-O bonds.

4 | CONCLUSION

In this paper, we analyze the structure and the explosion mechanisms of ZnCP. ZnCP as a popular primary explosive appears attracting stabilities and high energy. In the most stable structure, O atom and one of the terminal N atoms as the coordination atoms participate in forming the delocalized 5c-4e bond in the coordination structure. The weakest bond in ZnCP is Zn-N bond with the bond energy of 32.08 kcal/mol, which is the solicitation bond in the explosion. Three Zn-N bonds appear different WBI values and BDEs, which suggest the three-step mechanism in the decomposition.

As for the role of Zn^{2+}, the electronic structure suggests Zn^{2+} is a stabilizer in the complex under the ambient condition. But in the decomposition, Zn^{2+} is a catalyst and an anion-carrier in the explosion.

Different for the traditional viewpoints that the cleavage of coordinative bonds triggers the continuous decomposition, we prove it is a synergetic O transferring mechanism in the initial period and a stepwise mechanism for ring-opening in the midterm. The synergetic cleavage of Cl-O and Zn-N bond triggers the first ring-opening reaction and the continuous decomposition. The second ring-opening reaction is catalyzed by the neighbored Zn^{2+}. The third step of the ring-opening is caused by the weaker stability of $[Zn\text{-}CHZ]^{2+}$ with the departure of CHZ groups.

ZnCP is already applied in the modern industry caused by its special stability and the high energy content in the explosion. This study is a theoretical research to reveal how Zn^{2+} affects the explosion, which is a significant step to make clear the explosive mechanisms in primary explosives with different metals.

ACKNOWLEDGMENTS

The work is supported by the National Natural Science Foundation of China (NSFC 21701001), Anhui Provincial Natural Science Foundation (1708085QB42), China Postdoctoral Science Foundation (2018M632013), the State Key Laboratory of Explosion and Technology (ZDKT 17-01) and the Fundamental Research Funds for the Central Universities (2017cx10007).

ORCID

Kun Wang https://orcid.org/0000-0003-2175-1105
Longjiu Cheng https://orcid.org/0000-0001-7086-6190

REFERENCES

[1] J. Giles, *Nature*. **2004**, *427*, 580.
[2] M. H. V. Huynh, M. D. Coburn, T. J. Meyer, M. Wetzler, *PNAS*. **2006**, *103*, 10322.

[3] C. Zhang, C. Sun, B. Hu, C. Yu, M. Lu, *Science.* **2017**, *355*, 374.
[4] W. Zhang, J. Zhang, M. Deng, X. Qi, F. Nie, Q. Zhang, *Nat. Commun.* **2017**, *8*, 1.
[5] Q. T. Fan, Studies om imidazolium-based energetic compounds, Beijing Institute of Technology **2008**.
[6] Z. G. Zhang, Researches on Perchlorate Carbohydazide energetic coordination compounds, Beijing Institute of Technology **2000**.
[7] K. Wang, D. Zeng, J.-G. Zhang, Y. Cui, T. L. Zhang, Z. M. Li, X. Jin, *Dalton Trans.* **2015**, *44*, 12497.
[8] K. A. McDonald, S. Seth, A. J. Matzger, *Cryst. Growth Des.* **2015**, *15*, 5963.
[9] S. Y. Qi, Z. M. Li, T. L. Zhang, *Acta Chim. Sinca* **2011**, *69*, 138.
[10] J. Song, T. Zhang, J. Zhang, G. Ma, Y. Li, K. Yu, *Acta Chim. Sinica.* **2003**, *61*, 1444.
[11] M. B. Talawar, A. P. Agrawal, J. S. Chhabra, S. N. Asthana, *J. Hazard. Mater.* **2004**, *113*, 57.
[12] Z. R. Wei, T. L. Zhang, C. H. Lv, *Chinese J. Inorg. Chem.* **1999**, *15*, 482.
[13] J. G. Zhang, T. L. Zhang, Z. R. Wei, *Chem. J. Chinese U.* **2001**, *22*, 895.
[14] T. L. Zhang, B. D. Wu, L. Yang, Z. N. Zhou, J. G. Zhang, *Chinese J. Energ. Mater.* **2013**, *21*, 137.
[15] Y. H. Sun, T. L. Zhang, J. G. Zhang, *Chinese J. Inorg. Chem.* **2004**, *21*, 113.
[16] Y. Zhao, D. G. Truhlar, *Theor. Chem. Acc.* **2008**, *120*, 215.
[17] R. A. Kendall, T. H. Dunning, R. J. Harrison, *J. Chem. Phys.* **1992**, *96*(9), 6796.
[18] M. J. T. Frisch, G. W.; Schlegel, H. B.; Scuseria, G. E.; Robb, M. A.; Cheeseman, J. R.; Montgomery, J. A. Jr.; Vreven, T.; Kudin, K. N.; Burant, J. C.; Millam, J. M.; Iyengar, S. S.; Tomasi, J.; Barone, V.; Mennucci, B.; Cossi, M.; Scalmani, G.; Rega, N.; Petersson, G. A.; Nakatsuji, H.; Hada, M.; Ehara, M.; Toyota, K.; Fukuda, R.; Hasegawa, J.; Ishida, M.; Nakajima, T.; Honda, Y.; Kitao, O.; Nakai, H.; Klene, M.; Li, X.; Knox, J. E.; Hratchian, H. P.; Cross, J. B.; Bakken, V.; Adamo, C.; Jaramillo, J.; Gomperts, R.; Stratmann, R. E.; Yazyev, O.; Austin, A. J.; Cammi, R.; Pomelli, C.; Ochterski, J. W.; Ayala, P. Y.; Morokuma, K.; Voth, G. A.; Salvador, P.; Dannenberg, J. J.; Zakrzewski, V. G.; Dapprich, S.; Daniels, A. D.; Strain, M. C.; Farkas, O.; Malick, D. K.; Rabuck, A. D.; Raghavachari, K.; Foresman, J. B.; Ortiz, J. V.; Cui, Q.; Baboul, A. G.; Clifford, S.; Cioslowski, J.; Stefanov, B. B.; Liu, G.; Iashenko, A.; Piskorz, P.; Komaromi, I.; Martin, R. L.; Fox, D. J.; Keith, T.; Al-Laham, M. A.; Peng, C. Y.; Nanayakkara, A.; Challacombe, M.; Gill, P. M. W.; Johnson, B.; Chen, W.; Wong, M. W.; Gonzalez, C.; Pople, J. A., Gaussian 09, Wallingford, **2009**.
[19] M. D. Segall, P. J. D. Lindan, M. J. Probert, C. J. Pickard, P. J. Hasnip, S. J. Clark, M. C. Payne, *J. Phys.: Condens. Matter.* **2002**, *14*, 2717.
[20] J. P. Perdew, K. Burke, M. Ernzerhof, *Phys. Rev. Lett.* **1996**, *77*, 3865.
[21] H. J. Monkhorst, J. D. Pack, *Phys. Rev. B* **1976**, *13*, 5188.
[22] T. H. Fischer, J. Almlof, *J. Phys. Chem.* **2009**, *21*, 1.
[23] P. Giannozzi, S. Baroni, N. Bonini, M. Calandra, R. Car, C. Cavazzoni, D. Ceresoli, G. L. Chiarotti, M. Cococcioni, I. Dabo, A. D. Corso, S. d. Gironcoli, S. Fabris, G. Fratesi, R. Gebauer, U. Gerstman, C. Gougoussis, A. Kokalj, M. Lazzeri, L. Martin-Samos, N. Marzari, F. Maur, R. Mazzarello, S. Paolin, A. Pasquarell, L. Paulatto, C. Sbraccia, S. Scandolo, G. Sclauzero, A. P. Seitsonen, A. Smogunov, P. Umari, R. M. Wentzcovitch, *J. Phys. Condens. Matter.* **1985**, *55*, 2471.
[24] R. Car, M. Parrinello, *Phys. Rev. Lett.* **1985**, *55*, 2471.
[25] S. Nosé, *Mol. Phys.* **1984**, *52*, 255.

SUPPORTING INFORMATION

Additional supporting information may be found online in the Supporting Information section at the end of this article.

How to cite this article: Wang K, Dai C, Sun C, Cheng L, Zhang J, Zhang T. The effects of Zn^{2+} and ClO_4^- in the excellent primary explosive $Zn(CHZ)_3(ClO_4)_2$. *Int J Quantum Chem*. 2020;120:e26107. https://doi.org/10.1002/qua.26107